

# Evolution of Debris of a Tidally Disrupted Star by a Massive Black Hole: Development of a Hybrid Scheme of the SPH and TVD Methods

Hyung Mok Lee

Department of Earth Sciences, Pusan National University, Pusan 609-735, Korea

and

Sungsoo S. Kim

Institute for Basic Sciences, Pusan National University, Pusan 609-735, Korea

## ABSTRACT

The evolution of the stellar debris after tidal disruption due to the super massive black hole's tidal force is difficult to solve numerically because of the large dynamical range of the problem. We developed an SPH (Smoothed Particle Hydrodynamics) - TVD (Total Variation Diminishing) hybrid code in which the SPH is used to cover a widely spread debris and the TVD is used to compute the stream collision more accurately. While the code in the present form is not sufficient to obtain desired resolution, it could provide a useful tool in studying the aftermath of the stellar disruption by a massive black hole.

*Subject headings:* hydrodynamics – galaxies : nuclei

## 1. INTRODUCTION

The stars in the vicinity of the Super Massive Black Hole (SMBH), which is believed to exist at the center of galaxies, are disrupted by the SMBH's strong tidal force at a rate of one per  $10^{3\sim 4}$  yrs (e.g. Gooman & Lee 1989). It is very important to know the detailed evolution of the stellar debris because the amount of energy released as a result of stellar disruption depends on the way of evolution of the debris.

However, the numerical approach to this problem is very difficult. The debris forms a narrow, long stream in a wide area around the black hole. The incoming stream with short orbital periods collides with the outgoing stream because the orbits around a massive black hole do not form a closed ellipse. The precise evolution of the debris depends on the outcome of the stream collision which requires very high resolution studies. No single numerical scheme developed so far is able to handle this problem.

Cannizzo, Lee, & Goodman (1990) argued that the initial, extremely eccentric orbit of the stellar debris will form a circular disk after experiencing strong shocks which thermalize the orbital energy and studied the subsequent evolution of the accretion disk using a time-dependent  $\alpha$ -disk model. Kochanek (1994) studied the long-term evolution of the debris stream and predicted the geometry and physical properties when the stream collides with itself. However, the circularization argument by Cannizzo *et al.* (1990) and the results of Kochanek's (1994) analytical method remain to be numerically verified.

Numerical simulations for the evolution of the debris stream were done by Monaghan & Lee (1994) and Lee, Kang, & Ryu (1996). Although Monaghan & Lee (1994) used the SPH (Smoothed Particle Hydrodynamics) method to follow the evolution of the stellar debris in a huge space, the poor resolution due to a limited number of particles made a detailed study for the collision area impossible. On the other

hand, Lee *et al.* (1996) concentrated on the hydrodynamics of the collision area of the debris streams using the TVD (Total Variation Diminishing) scheme. They concluded that the stream-stream collisions are expected to circularize the stellar debris efficiently unless the ratio of the cross sections of the two streams is much larger than 10. However, the region of their simulation was restricted only to the collision area, and the gravitational force by the black hole was not included in the calculation because the entire volume of their simulation was very small.

There are usually two approaches to solve the hydrodynamics numerically: Lagrangian scheme and Eulerian scheme. The Lagrangian scheme is adequate for the problems with time-varying extent while Eulerian scheme is better fitted to the problem of limited extent. Lagrangian method is suitable to the overall spread of the debris but Eulerian scheme is a better choice for the description of stream collision. Thus we developed a hybrid scheme in the present paper to study the long term evolution of stellar debris. We have adopted Smoothed Particle Hydrodynamics (SPH) as a Lagrangian scheme and Total Variation Diminishing (TVD) scheme as an Eulerian scheme.

The SPH method was invented to simulate complex hydrodynamic phenomena in astrophysics (for the details of SPH method, see Monaghan [1992] and references therein). It is a particle method in which physical quantities are described with non-fixed particles. Spatial derivatives are calculated by analytical differentiation of interpolation formulae. Since the SPH is a particle method, it can handle spatially complex, wide-area physics more easily than finite-difference methods which are more accurate for some problems requiring high resolution.

The TVD method was originally developed by Harten (1983). It is an explicit, second-order, Eulerian finite-difference method which solves a hyperbolic system of the conservation equations. The key merit of this method is to achieve the high resolution of a second-order accuracy while preserving the robustness of the nonoscillatory first-order method.

This paper is organized as follows. Preliminary simulation using the SPH is first shown in §2, and the SPH-TVD hybrid procedure used in this study is described in §3. The simulation results performed with such a code are presented in §4. The discussions will be given in §5.

## 2. SOME RESULTS FROM THE SPH SIMULATIONS

A series of snapshots of an SPH simulation for the typical first encounter between a normal star and an SMBH is shown in Figure 1. The normal star here is modelled by a polytrope of index  $3/2$ . The mass of the SMBH,  $M_{\text{BH}}$ , is  $10^7 M_{\odot}$ , mass of the normal star is  $1 M_{\odot}$ , and the stellar orbit is chosen as a hyperbola with pericentral distance of  $1.5 \times 10^{13}$  cm with  $v_{\infty} = 10$  km/s. The tidal force by the SMBH is so strong that the normal star is completely disrupted and a long stream of the stellar debris is forming. This stream is even more stretched out as it returns to the SMBH for the second time as in Figure 2. The head of the stream is composed of the particles facing the SMBH when the star passes by the SMBH, and thus has smaller semi-major axes and periods than the tail. After the head passes by the SMBH for the second time, it collides with incoming stream as shown in Figure 3. However, the number of the SPH particles in the collision area in our simulation is too small for a precise hydrodynamic description. Our SPH simulation was done with 9185 SPH particles, and with a current CPU ability, it is not practicable to perform an SPH simulation with more than few tens of thousands particles. This shows the reason why the SPH alone is not able to handle this specific problem.

It is inevitable to use the SPH method at the beginning of the above calculation because the debris of the disrupted star is spread over a wide area, but a supplementary scheme is necessary to obtain a higher resolution in the collision area. For this reason, we set a TVD grid where hydrodynamically complex phenomena take place as in Figure 3, and conduct the calculation of the evolution of the debris using the TVD when an SPH particle comes into the TVD grid. The SPH is applied again for the material out of the TVD grid.

### 3. THE HYBRID CODE

Making a hybrid code out of conceptually different two numerical methods is not a trivial task. Physical quantities on the SPH-TVD border should be converted carefully from SPH to TVD and TVD to SPH, conserving energies and other physical quantities. Although it is quite straightforward to convert from the SPH to the TVD, the reverse procedure requires a bit of numerical consideration to keep the number of created particles small enough for the whole run.

When the SPH particles approach pericenter for the second time, due to a limited number of the SPH particles, the resolution length of those particles is so large that the incident flux to the TVD box fluctuates unrealistically. Therefore, we take time-averages for the flux of incoming SPH particles and artificially create incoming particles with a constant flux at the SPH-TVD border. Since the period of our whole run is short compared to the orbital period of the very tail of the stream, the incoming flux may be assumed to be a constant. (The actual incoming flux varies like  $t^{-5/3}$ ; see, for example, Rees [1988].) Then the conversion from SPH to TVD is done with such artificial SPH particles, and we will call this procedure SPH2TVD. Detailed procedure is discussed in §3.1.

Now the quantities mapped onto the TVD grid are calculated with the TVD code. For the TVD part, we adopted the code written by Lee *et al.* (1996). A modification to the original code is explained in §3.1.

The time step for the TVD calculation is determined by the velocity of the fluid in the TVD box. Although the speed of the stream reaches a maximum at the closest point to the SMBH, hydrodynamic effects near the SMBH may be neglected because the pressure force is much smaller than the tidal force and gravitational force. Thus by locating the SMBH outside the TVD box and calculating the motion of the fluid as a collection of free-streaming-particles (particles with no hydrodynamics), one could save large amount of CPU time and memory. For this reason, we put the TVD box that encompasses the collision area only (apart from the SMBH), and at the TVD border facing the SMBH, we convert the TVD quantities into SPH particles without considering hydrodynamics. We will call this procedure TVD2SPH, and the details of this procedure are given in §3.2.

After the SPH particles that are created at the TVD border facing the SMBH, they revolve around the SMBH and enter the TVD box for the second time. This step is identical to the SPH2TVD procedure above.

Finally, the stream collides with its own tail in the TVD box, where the hydrodynamics is calculated with a higher resolution using TVD method.

It was found that the sequence of the above procedures is important in determining the accuracy and consistency of the whole simulation. The sequence which gives the best result would not be only one, but we find that the total energy is conserved the best when we make the code with the following sequence:

Step 1. TVD2SPH : Conversion of physical quantities from TVD grids to SPH particles.

Step 2. TVD : TVD calculation.

Step 3. SPH : SPH calculation.

Step 4. SPH2TVD : Conversion from SPH particles to TVD grids.

Step 5. SPH stacking : Keeping the number of SPH particles small.

Step 6. Output : Making various outputs.

Step 7. Time step : Determining the time step.

Step 8. Go to Step 1.

In Step 7, the time step of the code is usually determined by the TVD part since it requires a smaller time step than other procedures. Then the SPH quantities are advanced by one time step by integrating the equation of motion over one time step. Steps 1 and 4 will be discussed below in detail.

### 3.1. Conversion from SPH to TVD

The initial phase should be calculated by using the SPH where fluid element is represented by a collection of particles. We need to convert the particle variables into field variables at grid points in order to perform TVD calculations where high spatial resolution is required. The conversion is automatically carried out by the SPH part in the following manner:

$$\begin{aligned}\rho(x, y, z) &= \sum_i m_i W(r, h) \\ \rho(x, y, z) \mathbf{v}(x, y, z) &= \sum_i m_i \mathbf{v}_i W(r, h) \\ u(x, y, z) &= \sum_i m_i E_{th,i} W(r, h),\end{aligned}\tag{1}$$

where  $\rho$  is the density,  $m_i$  is the mass of the  $i$ -th particle,  $u$  is the thermal energy per unit volume,  $E_{th}$  is the thermal energy per unit mass of the particle, and  $W(r, h)$  is the spherical interpolation kernel with resolution length  $h$ . As for  $W(r, h)$ , we have adopted the spline based kernel in our code. The only remaining problem is how to choose the grid size. In order to determine the optimal grid size we made a few experiments. In Figure 4a, we have shown the density contour of an unperturbed main-sequence star of polytrope of  $n = 3/2$  realized by particles using SPH and mapped onto cubical grids of the size equivalent to the resolution length. It is clear that the grid size is too large to represent the low density region in the outer parts of the star. Thus we need to choose the grid size smaller than the resolution length  $h$  in order to have an accurate and realistic density distribution. Increasing the number of grid points by a factor of 4 on each side gave an adequate representation as shown in Figure 4b. Repeated experiments showed that the grid size should be at least four times smaller than the SPH's resolution length.

Since the original TVD program that we adopted did not have the external gravitational field, we have modified the equation of motion to take into account the relativistic gravitational field as follows.

Step 1. Compute  $\phi^n$  from the velocity field  $v_i^n$  at the grid points. The velocity comes in because of the relativistic correction, for which we adopted the following post-Newtonian formula

$$\phi = GM_{\text{BH}} \left( -\frac{1}{r} + \frac{1}{2r^2} + \frac{3v^2}{2r} + \frac{3v^4}{8} \right).\tag{2}$$

Step 2. Estimate the new velocity that takes into account the effect of external gravitational field: i.e.,

$$v_i^n = \tilde{v}_i^n + \frac{1}{2} \frac{\partial \phi^n}{\partial x_i}, \quad (3)$$

where  $\tilde{v}_i^n$  is the velocity field in the absence of external gravity.

Step 3. Make corrections of hydrodynamical force computed by the TVD:

$$\begin{aligned} \rho^{n+1} &= \rho^n + \Delta \rho^{TVD}(\rho^n, \tilde{v}_i^n, \tilde{P}^n) \\ v_i^{n+1} &= v_i^n + \Delta \rho^{TVD}(\rho_i^n, \tilde{v}_i^n, \tilde{P}^n) \\ P^{n+1} &= P^n + \Delta P^{TVD}(\rho^n, \tilde{v}_i^n, \tilde{P}^n), \end{aligned} \quad (4)$$

where  $P$  is the pressure, and  $\tilde{P}$  the pressure in the absence of external gravity.

Step 4. Recompute the external potential in the middle time step using the estimated velocity at the middle time step:

$$v_i^{n+1/2} = \frac{v_i^n + v_i^{n+1}}{2} \rightarrow \phi^{n+1/2}. \quad (5)$$

Step 5. Finally, we compute the velocity field and gravitational potential at the  $n+1$ -th step using the velocity field at the mid step above.

$$v_i^{n+1} = v_i^{n+1/2} + \frac{\partial \phi^{n+1/2}}{\partial x_i} \frac{dt}{2}. \quad (6)$$

In the above procedure, the effect of the black hole's gravity is computed up to  $(\Delta t)^2$ . In the vicinity of the black hole, the acceleration is completely dominated by the black hole and it is important to account for the black hole gravity very accurately.

### 3.2. Conversion from TVD to SPH

The quantities of one SPH particle are usually mapped onto several vertices of the TVD grid. The number of mapped TVD vertices depends on the size of the resolution length of the SPH particle. On the other hand, the inverse mapping is not mathematically unique since the location and the mass of particles cannot be simultaneously determined. It would be possible to create SPH particles at every TVD vertex on the boundary, but there would be too many SPH particles. We have tested possibility of creating SPH particles by summing up the quantities of  $2^3$  or  $3^3$  TVD vertices. By doing this, we were able to decrease the number of created SPH particles by a large factor, but the gravitational potential energy was not well conserved because the strong gravitational force by the SMBH made a small positional error during the summing-up process and resulted in a quite large potential energy discrepancy. Thus, we concluded that the SPH particles have to be created at each TVD vertex. In order to reduce the number of SPH particles to a manageable level, we did not create a particle if the density in a cubical grid is smaller than  $10\rho_{min}$ , where  $\rho_{min}$  is the density of the ambient medium (i.e., vacuum) in TVD program. We used  $\rho_{min} \approx 10^{-4}\bar{\rho}$  where  $\bar{\rho}$  is the mean density of the stream. Also the particle creation was done only for the case where the mean flux at the cubical grid is directed outward. Similarly, the velocity and thermal energy of the newly created particles are determined by the flux and thermal energy density of the corresponding TVD vertex.

## 4. SIMULATION

### 4.1. Parameters

We calculated the evolution of the debris of the tidally disrupted star by an SMBH using our hybrid code developed in this study. Only SPH is used for the calculation until right after the tidal disruption, and the TVD part starts when the particles with shorter orbital periods return to the vicinity of the black hole for the second time. The physical parameters chosen in this simulation are identical to those given in §2. The natural units used here are  $GM_{\text{BH}}/c^3 \simeq 49$  sec for the time,  $GM_{\text{BH}}/c^2 \simeq 1.48 \times 10^{12}$  cm for the length, and  $M_{\text{BH}}$  for the mass.

The size of the TVD grid is  $180 \times 250 \times 80$ , and the distance between vertices is 0.5 code length unit. The TVD box was located such that the stream-stream collision takes place at the center of the box as shown in Figure 3.

### 4.2. Results

Figure 5 is a series of density contour snapshots of our simulation. The contour lines are drawn at every increment by a factor of 10. At  $it = 1500$ , where  $it$  is the time step index, an unperturbed stream enters into the TVD box indicated by the inner box. At  $it = 1800$ , the stream passes by the SMBH whose location is indicated by a ‘+’ sign. The first collision occurs at around  $it = 2100$ . At  $it = 2400$ , the incoming stream does not seem to be much perturbed by the collision with the very top of the stream’s head. Instead, the head of the outgoing stream is reflected by the incoming stream and progresses in the opposite direction to the incoming stream because the expansion of the outgoing stream during the second revolution around the SMBH makes the density of it lower than the incoming stream by a factor of a few tens. This expansion is caused by the finite size of the stream which has been set somewhat arbitrarily in this study, and will be discussed in more detail in §5. The effects of the collision on the incoming stream clearly appear as a perpendicular velocity component in it from  $it = 2700$  (see discussions below). The outer contour lines of the stream are not smoothly connected at the SPH-TVD boundary at  $it = 2700$  and 3000, because the SPH particles are not created for TVD vertices with low densities, as discussed in §3.2. We have stopped our calculation at  $it = 3000$ .

The velocity field at  $it = 2700$  is shown in Figure 6. The lengths of the arrows are proportional to the flux-averaged velocity over the z-axis. It clearly shows that the low-density outgoing stream is reflected by the high density barrier of the incoming stream and that a part of the incoming stream is pushed away to the opposite side of the collision. It is interesting to note that the outgoing tenuous material has nearly uniform velocity field (very close to the positive y-axis). This is because the reflected matter exerts ram pressure to the following material. If the stream were very thin, then it would have not expanded after revolving around the SMBH. The collision point would be (10,140) (if one neglects the Lense-Thirring precession). However, since the stream does have a finite thickness and thus expands after revolving around the SMBH, the collision is not limited in a small region. Furthermore, first-colliding matters give following matters pressures toward positive x-axis direction. This causes the collision area even larger and the tail-to-head density ratio at the collision area becomes bigger. The conversion efficiency from kinetic energy to thermal energy becomes weak if the density ratio becomes large.

Density and pressure profiles along x-axis at  $Y \simeq 90$  for  $it = 1800$ , 2400, and 2700 are shown in Figure 7. The density is summed over the z-axis and the pressure is flux-averaged over the z-axis. At  $it = 1800$ ,

the density profile is nearly symmetric, but the pressure profile is inclined to the outside (in view of the SMBH). This is because the gravitational field of the SMBH is so strong that a small positional difference makes a non-negligible velocity shear. This effect is stronger at the side closer to the SMBH. The location of the collision may be found at the pressure peaks at  $it = 2400$  and  $2700$ . Although the tail-to-head density ratio is about  $10^2$  at these steps, the ram pressure of the head is strong enough to push the tail toward the negative x-axis: between  $it = 1800$  and  $it = 2700$ , the peak of the tail's density has been shifted by approximately 2 code length units. This shift will move the collision point outward when the shifted matter collides its tail later, making the collision area gradually wider again.

## 5. Discussion

The major effect of the supersonic stream collision is transferring the orbital energy into thermal energy which eventually becomes expansion energy of the shocked region. Although it has been seen in Figure 6 that the ordered velocity component has changed into somewhat random component, only a small amount of kinetic energy has been converted into thermal energy ( $\sim 2\%$ ; see Figure 8). We obtain such a low conversion efficiency because the tail-to-head density ratio at the collision region was as large as 100. The major effect of such collision is a reflection of a lower density stream by the high density stream.

As discussed in the previous section, the expansion of the outgoing stream in the early stage is due to the finite thickness of the stream: the thicker the stream, the bigger the expansion. Kochanek (1994) argued that there is a focal point near the SMBH where the thickness of the stream becomes infinitesimal. If this is real, the density ratio at the collision region may be close to unity and the collision may be more effective in converting kinetic energy into thermal energy. However, since the resolution of our TVD grid is of order of the thickness of the stream, such a focal point could not be realized in our simulation. To accomplish a resolution suitable for this phenomenon, we need to increase the number of the TVD grids by a factor of at least  $5^3$ , which is of course nearly impossible with a current CPU and memory limit. Thus, the significance of our simulation presented here is rather in making a smoothly working hybrid code out of two conceptually different numerical methods.

However, the results of our simulation give some insights in predicting the evolution of the stellar remnant. Since even with our coarse TVD grids, the shift of the incoming stream by the ram pressure of the outgoing stream was observed. This indicates that the shifted tail will revolve around the SMBH with a slightly different phase angle and will eventually collide with following stream at farther distance from the SMBH. The results of the collision with the stream with a new phase angle will depend on the amount of the phase angle shift and thickness of the stream. Generally, the phase angle change will result in larger density ratio at the collision area, making the collision less efficient in converting kinetic energy into thermal energy. If the phase angle change induces a change in the density ratio at collision in a much shorter time scale than the time for returning to the SMBH for the second time of the very tail of the stream, the collision of the streams will take place intermittently as suggested by Lee *et al.* (1996).

The accuracy of our code may be measured with the degree of the conservation of total energy. The relative total energy at each time step is plotted in Figure 8. Until the end of our simulation, the relative total energy is well conserved by less than 2%. The increments of the relative total energy between time steps 1400 and 1700, and between time steps 2200 and 2700 are caused by the inaccuracy in the TVD calculation probably due to coarse grids, not by the interfaces between SPH and TVD. In fact, the conversions from the TVD to SPH and SPH to TVD take place after  $it = 1700$ , and the error remains to

be very small after  $it = 1700$ , when the conversion from the TVD to SPH starts, until the thermal energy created in the coarse TVD box becomes important.

Our calculations assumed only gas pressure. However, the hot gas in the shocked region could be dominated by radiation pressure. If we still keep the adiabatic assumption but assumes the radiation pressure to dominate, the adiabatic index would be  $4/3$ . If the radiation energy loss becomes important, the shock becomes isothermal. However, the ignorance of radiative cooling would not be so critical during a very short period like ours presented here. Moreover, it is possible that the radiation loss is not important because of the high opacity for the radiation behind the shock. If so, the radiation is simply trapped by the thick medium.

Although it is very difficult to include radiation processes in the simulation like the one presented here, it is important to account these effects in order to predict the observational implications. The stellar disruption could release significant energy for extended periods through the accretion onto the black hole. The stream collision phenomenon could provide a short-lived activity in galactic nuclei. All these require more accurate understanding of stellar disruption.

This work was supported by the Cray R&D Grant in 1995. H. M. L. was supported in part by Basic Science Research Institute Program to Pusan National University under grant No. BSRI 95-2413.

## REFERENCES

- Cannizzo, J. K., Lee, H. M., & Goodman, J. 1990, ApJ, 351, 38
- Goodman, J., & Lee, H. M. 1989, ApJ, 337, 84
- Harten, A. 1983, J. Comp. Phys., 49, 357
- Kochanek, C. S. 1994, ApJ, 422, 508
- Lee, H. M., Kang, H., & Ryu, D. 1996, ApJ, 464, 131
- Monaghan, J. J. 1992, ARA&A, 30, 543
- Monaghan, J. J., & Lee, H. M. 1994, in The Nuclei of Normal Galaxies, NATO ASI Series C:445, eds. R. Genzel & A. I. Harris, (Kluwer), p453
- Rees, M. J. 1988, Nature, 333, 523
- Ryu, D., Ostriker, J. O., Kang, H., & Cen, R. 1993, ApJ, 414, 1



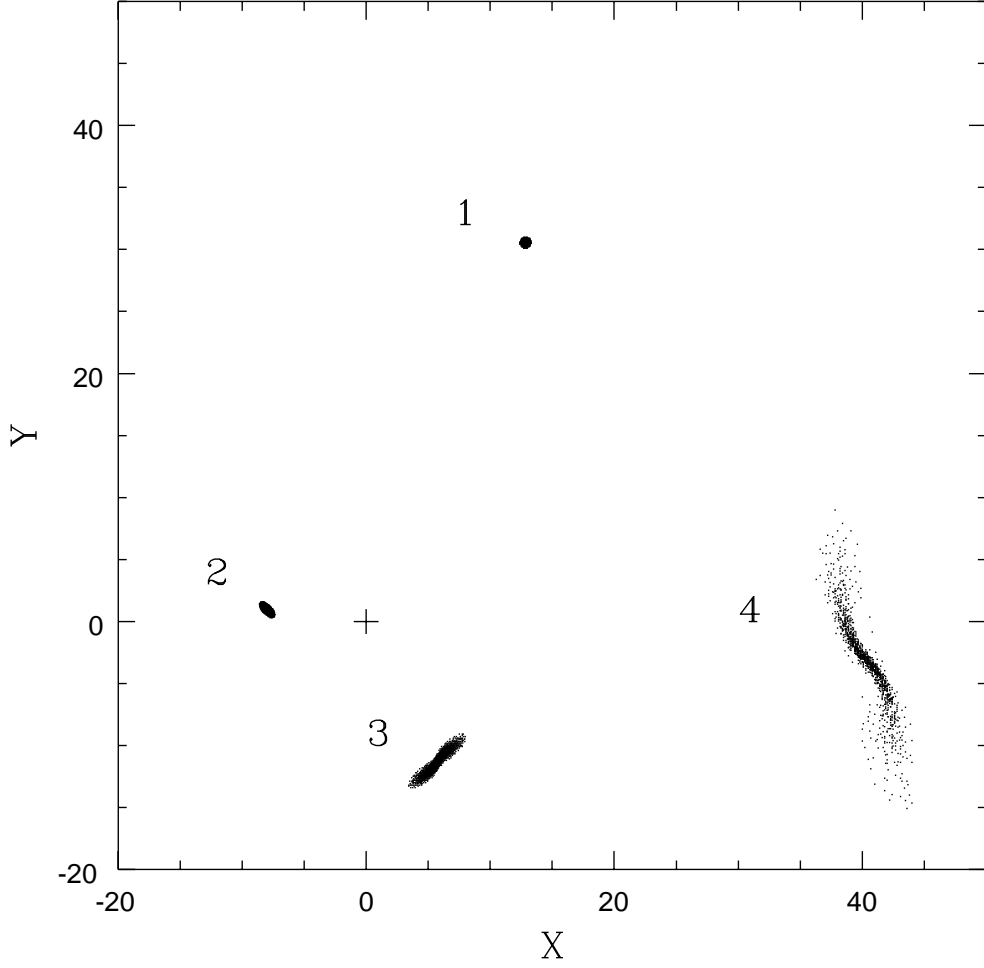


Fig. 1.— Four snapshots of initial SPH simulation for the encounter between an SMBH and a normal star. The location of the SMBH is indicated with a + sign, and the normal star is being disrupted by the strong tidal force of the SMBH. The sizes of the stars are increased by a factor of 10 and the length is in  $1.48 \times 10^{12}$  cm. See the text for simulation parameters.

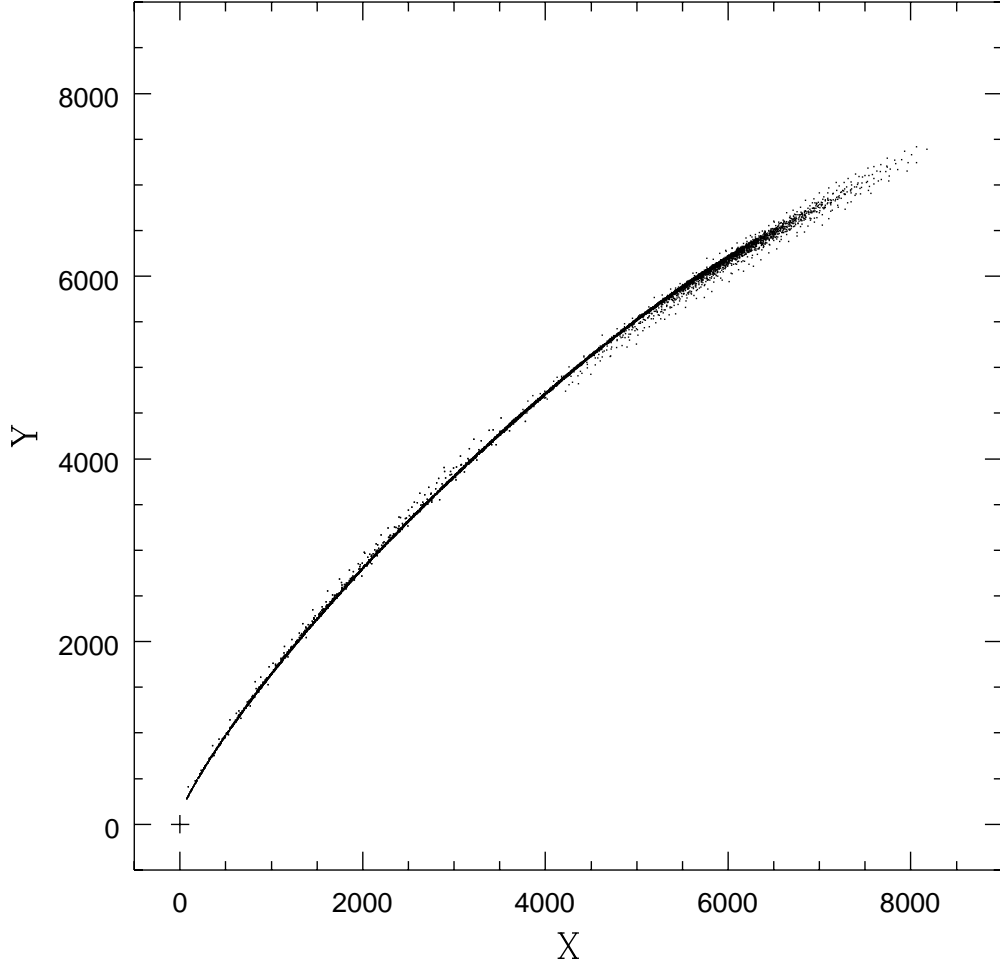


Fig. 2.— Stream of the stellar debris disrupted by the SMBH. The disrupted normal star in Figure 1 now forms a long, thin stream as it passes the apogee, and is approaching near the SMBH for the second time. The length unit is the same as in Figure 1.

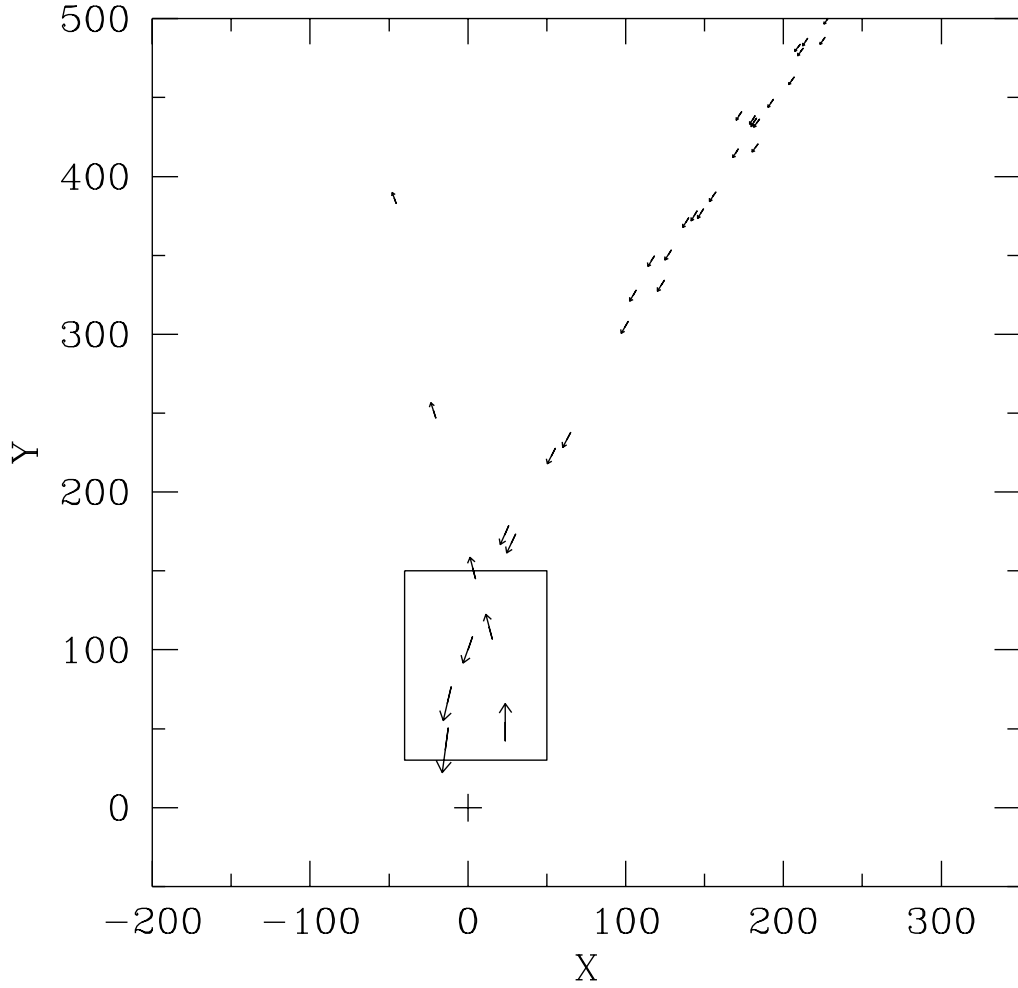


Fig. 3.— A leading part of the stream of the stellar debris disrupted by the SMBH. The head, which already passes by the SMBH for the second time, collides with its tail near (10,140). The number of SPH particles at the collision area is obviously too small for a precise hydrodynamic calculation. We put a TVD box (represented by the inner box) near the collision region to perform a precise hydrodynamic calculation for the collision with the TVD scheme, whose accuracy is better for this kind of situation than that of the SPH method. The length unit is the same as in Figure 1.

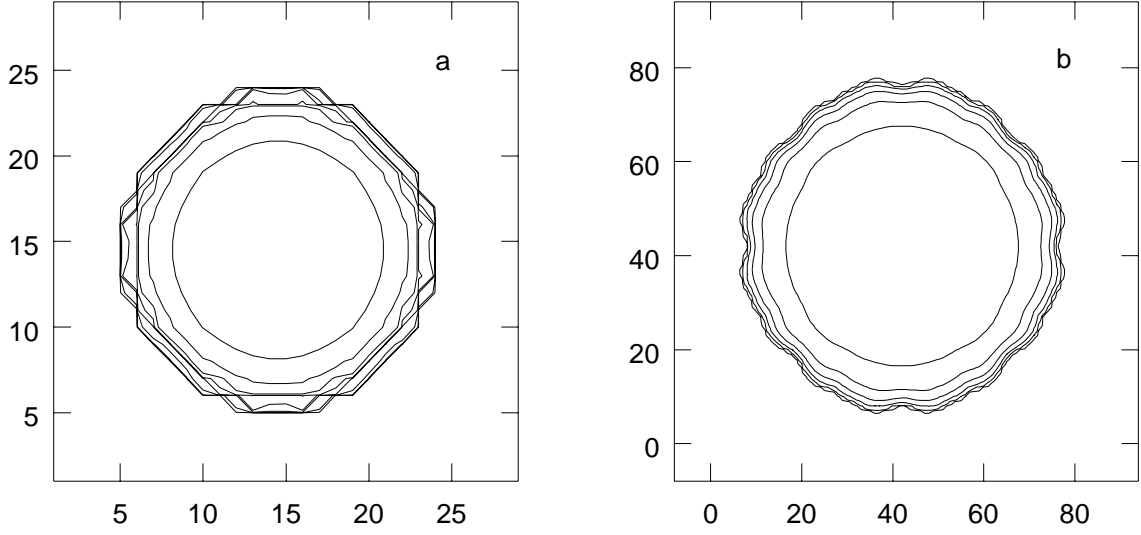


Fig. 4.— Density contour maps generated by mapping a normal star realized with a polytropic index of  $3/2$  with 9185 SPH particles into the TVD grids using interpolation kernel with (a) grid size  $= h$ , and (b) grid size  $= h/4$ , where  $h$  is the resolution length of the interpolation kernel. To nicely map the SPH particles into the TVD grids down to the region with a very low density, the grid size should be less than the resolution length of the SPH interpolation kernel.

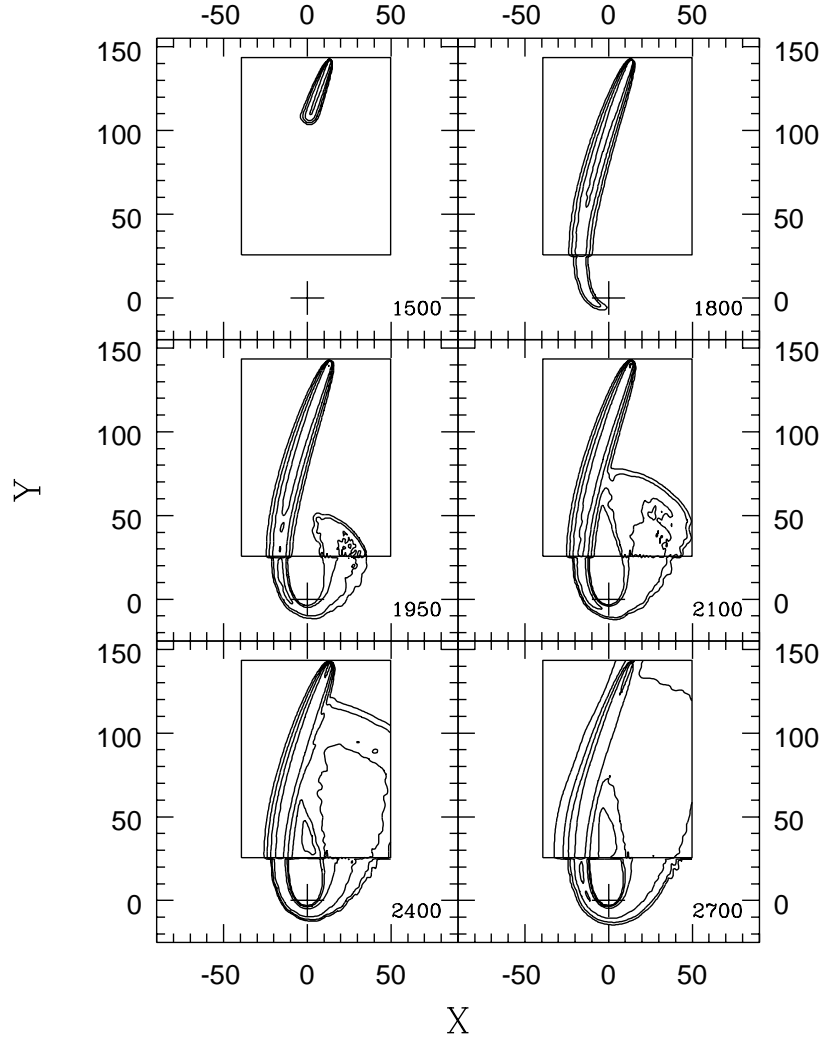


Fig. 5.— 6 density contour maps of the results of TVD-SPH hybrid simulation for the evolution of tidally disrupted stellar debris by the SMBH. The inner boxes represent the TVD box, in which the calculation is done with the TVD scheme. The number of TVD grid points for this simulation is  $180 \times 250 \times 80$ , and the length is in  $1.48 \times 10^{12}$  cm. Total duration of this simulation is about 30 hours.

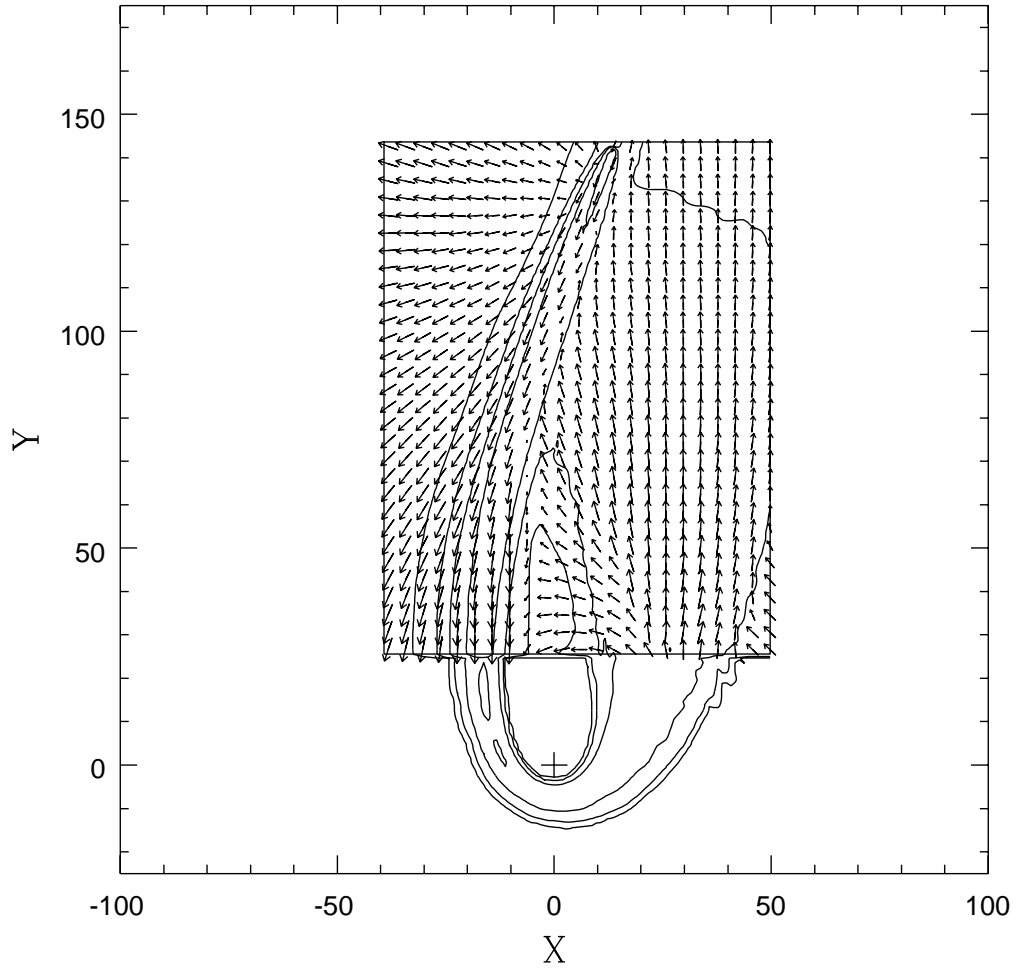


Fig. 6.— Velocity field of our simulation at  $it = 2700$ . The velocity has been density-averaged over the  $z$ -axis. The result of the stream collision is more of a reflection than a merger.

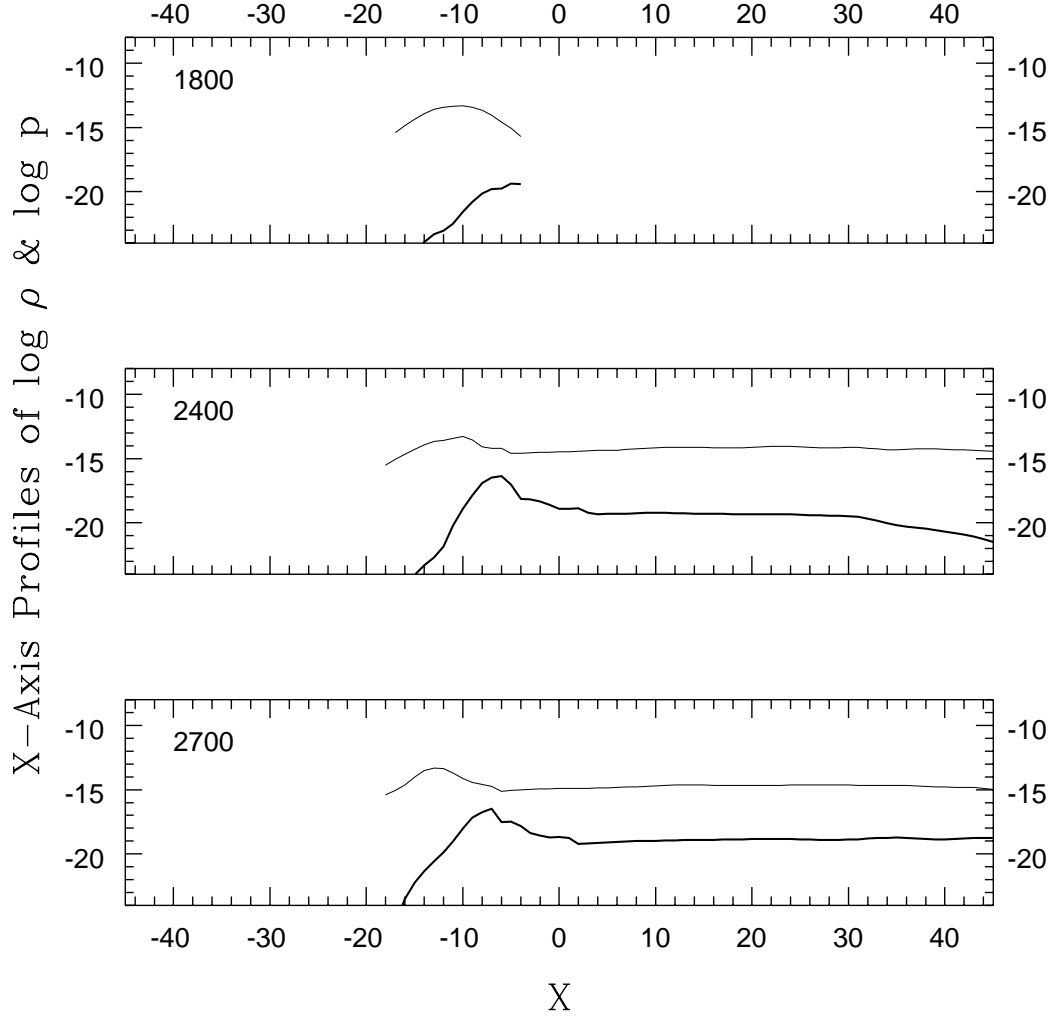


Fig. 7.— X-axis density (thin lines) and pressure (thick lines) profiles at  $Y \simeq 90$  at  $it = 1800$ ,  $2400$ , and  $2700$ . The pressure is density-averaged over the  $z$ -axis. Densities and pressures are in code units. (See the text for the code units.)

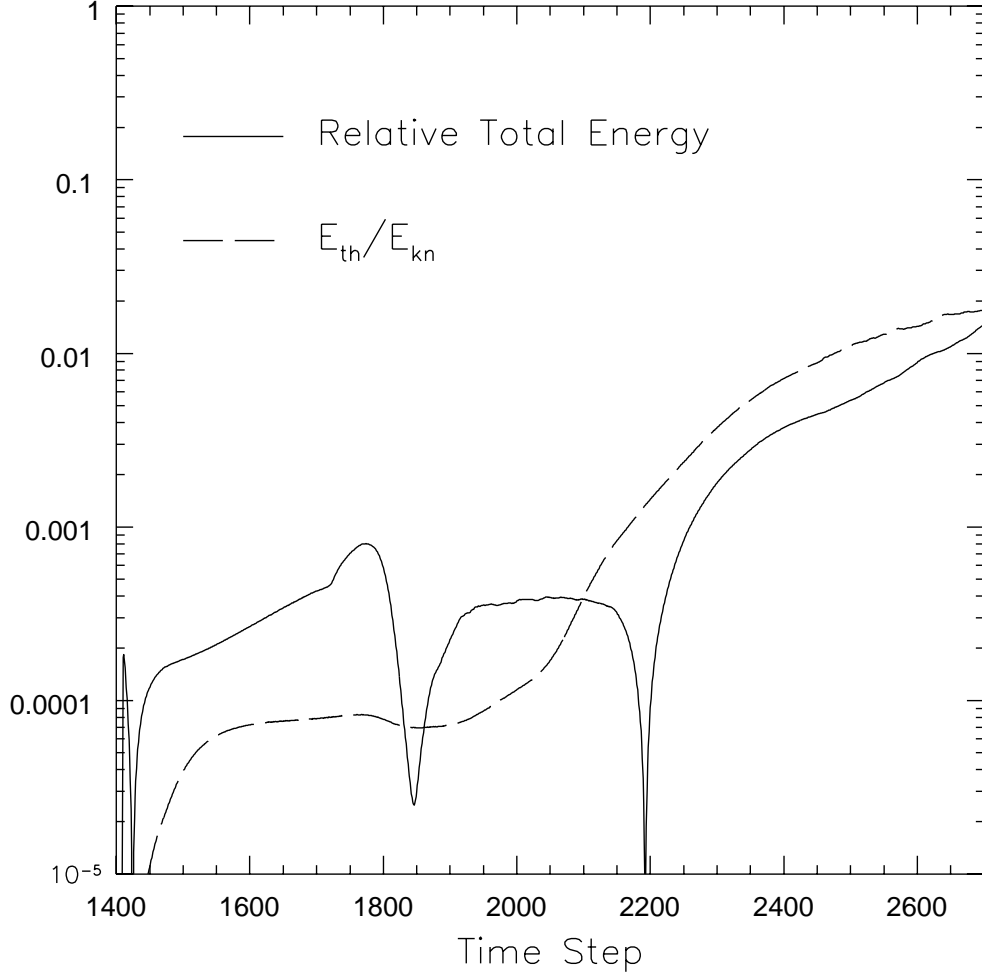


Fig. 8.— Temporal evolution of the relative total energy and the ratio of thermal energy to kinetic energy. The relative total energy is defined as  $(E_{gp} + E_{kn} + E_{th})/(|E_{gp}| + E_{kn} + E_{th})$ , where  $E_{gp}$  is the gravitational potential energy,  $E_{kn}$  the kinetic energy, and  $E_{th}$  the thermal energy. The relative total energy is lower than 0.02 for whole simulation, indicating that the accuracy of the code is acceptable. The main source of the inaccuracy is found to come from the coarseness of the TVD grids, not the interfaces between the SPH and TVD.